Method for image segmentation based on an encoder-segmented neural network and its application

Ning Li,* MEMBER SPIE
Youfu Li
City University of Hong Kong
Department of Manufacturing Engineering and Engineering Management
Kowloon
Hong Kong
E-mail: meyfli@cityu.edu.hk

Abstract. An Encoder-Segmented Neural Network (ESNN)-based approach is proposed to improve the efficiency of image segmentation. The features are ranked according to the encoder indicators by which the insignificant features will be eliminated from the original feature vectors and the important features reorganized as the encoded feature vectors for the subsequent clustering. The ESNN developed can improve on the existing Fuzzy c-Means (FCM) algorithm in feature extraction. The cluster number selection can be accomplished automatically. This method was successfully implemented for automatic labeling of tissues in MR brain images. Experimental results show that the ESNN-based approach offers satisfactory performance in both efficiency and adaptability.
 [S0091-3286(99)01905-4]

Subject terms: image segmentation; clustering; neural networks; feature extraction; Magnetic Resonance Imaging (MRI).

Paper 980233 received June 15, 1998; revised manuscript received Dec. 2, 1998; accepted for publication Dec. 9, 1998.

1 Introduction

Image segmentation is a very critical component in image processing because errors at this stage influence image understanding and pattern recognition. Various efforts have been made in the research[1] including the use of clustering for extracting information available out of the feature space without a priori knowledge. It has been proved that using image classification for segmenting multispectral images can improve the degree of confidence in the performance of segmentation compared to gray-scale approaches using single images.[2] Multidimensional data classification has been used extensively in the field of remote sensing.[3] Studies have reported on supervised and unsupervised pattern recognition techniques for multispectral data segmentation.[4,5] Many segmentation techniques have been developed on region-based segmentation using feature vector clustering such as the IOSDATA adopted by Ball and Hall[6] and the adaptive c-means clustering algorithm.[7] Although these studies have shown that some results are in visual agreement with an expert's judgment, a number of factors may reduce the feasibility and applicability of the classifiers.

The number of features needed depends on the complexity of the image. This is a crucial problem for using clustering in determining the constituents of the feature vector. High-dimensional feature spaces can yield improved performance on image segmentation, but the segmentation suffers from low computation efficiency. Although some approaches using neural networks have been proposed, the computational load still tends to be high if a large number of neurons are required for processing a large sized image.[8] Multispectral image segmentation requires each pixel be classified as reliably as possible with respect to the true class to which it belongs. Each useful feature plays an important role in the segmentation, but the contribution of each feature differs depending on the type of the image. The other problem is the automatic determination of the number of clusters. A segmentation algorithm must include some means for determining the number of classes from the data. Unfortunately, the number of clusters is required by clustering but is unknown in advance when segmenting an image. A large number of clusters will result in an oversegmented image, while too few clusters will result in improper clustering of dissimilar feature vectors.

In this paper, a novel Encoder-Segmented Neural Network (ESNN) is constructed based on vector quantization and Fuzzy c-Means (FCM) clustering for adaptive segmentation.[9] The proposed approach has unique characteristics differing from the conventional approach. The Self-Organized Feature Map (SOFM) is applied for analyzing the selected features. According to the contribution of each feature, the feature encoder is designed to determine a suitable feature vector for enhancing the performance of clustering for segmentation. The development of the FCM algorithm based on the encoded feature vector, called the EFFCM algorithm, reduces the amount of sample data needed for training, speeding up the computation. The sample data with the encoded feature vectors are clustered as the fuzzy membership functions of each class and then labeled into the relevant class in which the vector's membership function has the maximum contribution. The experiments indicate that by applying ESNN in MR brain image segmentation we can distinguish different tissues correctly and can also identify tumors when processing the

*On leave from Nanjing University of Aeronautics and Astronautics, Nanjing, China.

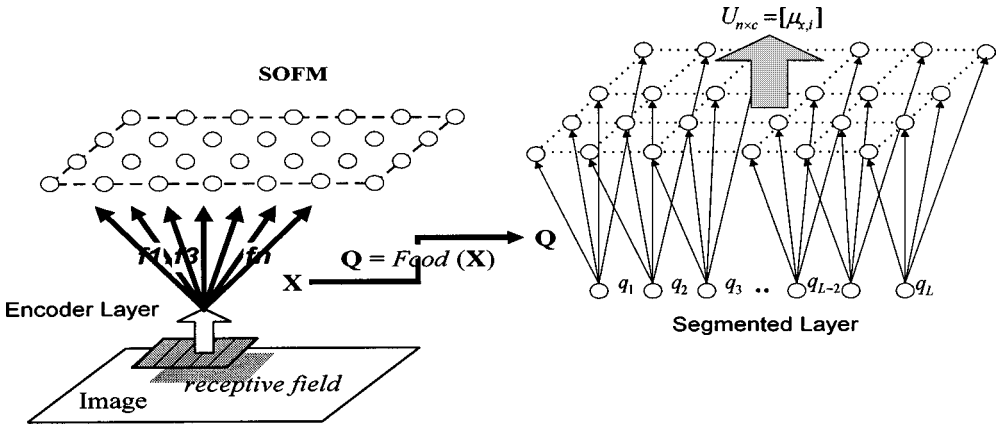

Fig. 1 The architecture of ESNN.

abnormal MRI by selecting the number of clusters appropriately. Quantitative evaluations and comparisons with other methods show that the developed ESNN method outperforms the FCM method by about 31% in segmenting MR brain images. With the ESNN method, satisfactory performance is achieved in the uniformity measurement. The computation efficiency is high compared with conventional clustering for processing a large number of patterns with multidimensional feature vectors.

In Sec. 2, we introduce the concept of ESNN for image segmentation in two parts: the feature encoder and the EFFCM algorithm for final segmentation. In Sec. 3, we describe the application of ESNN to segment MR brain images. The experimental results are shown through feature maps, tables, and pseudocolor images, followed by discussions on the performance of ESNN for segmentation. The conclusion is given in Sec. 4.

2 The Encoder-Segmented Neural Network (ESNN)

The ESNN here consists of two layers of networks as shown in Fig. 1. The first layer, the encoder, is used to train the feature vectors extracted from the input image using competitive learning. Mapping from feature space to spatial space is represented in the output neuron space by the SOFM. According to the weights associated with each connection between each feature and each neuron in the output space, the features can be encoded in a definite sequence for indicating the contribution of each feature to the clustering. Analyzing the definite sequence, some features can be removed in subsequent clustering due to the weak effect on clustering. The second layer, the segment, is implemented by the EFFCM algorithm. Each pixel that can be viewed as a point in the encoded feature space is then clustered into a particular class by minimizing an object function. The clustering result is represented as a fuzzy membership function by a matrix that represented the contribution of each pixel to each class. Each pixel in the input image is then labeled into the corresponding region represented as a color code if its membership function has a value larger than others. The computational procedure of ESNN for image segmentation is illustrated in the flow chart shown in Fig. 2.

2.1 *Feature Encoder by Self-Organizing Feature Map (SOFM)*

Vector quantization based on Kohonen's self-organizing network has a number of advantages in feature extraction for segmentation. A neural network is naturally oriented toward a highly parallel computing architecture so as to decrease the complexity of computation. An adaptive neural network training algorithm, such as Kohonen's SOFM, frequency sensitive competitive learning algorithm, and near-optimal competitive learning algorithm,[10–12] can promise greater flexibility in the design of vector quantization. However, the SOFM does not guarantee preservation

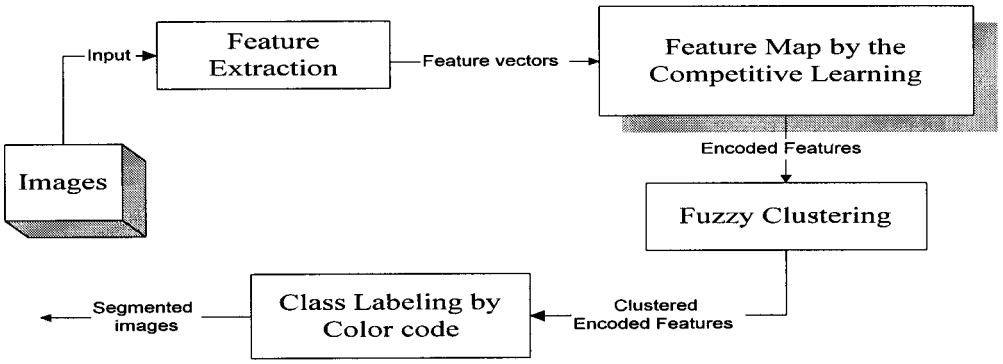

Fig. 2 Block flow diagram of image segmentation by the ESNN.

of exact connectivity relationships between clusters or regions. It can provide the topological neighborhood relationship in the input feature space to the greatest extent. In other words, the feature map can reflect the contribution of the input feature vector to clustering via the distribution of the neurons in the output layer. Thus, we construct the ESNN and use the SOFM for the feature encoding.

The feature encoder consists of a number of feature vector units in the input layer and a feature map unit in the output layer. Each neuron of the input layer representing one of the selected features has its weights associated with the connections from itself to each neuron of the output layer. To reduce the computational burden due to the large number of pixels in an image, only pixels in a receptive field, fixed by a movable nonoverlapped window,[13] are processed from the original image. For different sized images, the window can have different sizes. The output layer is $p \times q$ neurons in a two-dimensional space. The network is trained by the self-organizing competitive learning algorithm. During the training, only one of the neurons in the output layer, the winner, is activated at a time determined by the minimal distance criterion and then assigned into the appropriate class. The others are prohibited. Thus, the weights of the winning neuron and its neighborhood are updated with all the others unchanged. The appropriate weights can be modified by the Kohonen learning rules:

$$w_{ij}(t) = w_{ij}(t-1) + \eta(t,i)\Lambda(i,i^*,t)\sum_{j=1}^{n}[f_j^t - w_{ij}(t-1)] \quad \text{for } j=1,2,...,n; \quad i=1,2,...,N, \tag{1}$$

where $\Lambda(i,i^*,t)$ is the neighborhood function for the winner i^*, $\eta(t,i)$ is the learning rate function for the i'th neuron, and f_j^t is the j'th feature of the input vectors. The training process continues until the encoder network converges when the cost function $E(t)$, called the Lyapunov $\boldsymbol{E}$, defined in Eq. (2), is minimized:

$$E(t) = -\frac{1}{2}\sum_{ij}\sum_{\mu=1}^{n}\Lambda(i,i^*,\mu)[x_i^\mu - w_{ij}(t)]^2, \tag{2}$$

where x_i^μ stands for the input feature vectors.

After training, mapping from feature space to spatial space can be built via the SOFM by spatial self-organization. Thus, the contribution of the input feature vectors to clustering can be depicted vividly by the SOFM and can be represented by its weight vectors. For $p \times q$ neurons in a two-dimensional output layer of the feature encoder network, all the weights W_{ij}, associated with a connection from the j'th feature to i'th neuron, are fixed and the contribution of features is shown in the output neurons of the SOFM. If the neurons have similar contribution, they will be clustered so that several regions will be produced in the SOFM.

We define an encoded feature parameter, A_f^c to present the contribution of the feature f to all the neurons within region c in the feature map. This parameter is calculated from the related weights as follows:

$$A_f^c = \frac{1}{r_c}\sum_{i=1}^{r_c} w_{if} \quad f=1,2,...,p; \quad c=1,2,...,k, \tag{3}$$

where r_c denotes r neurons in region c and w_{if} is the weight associated with one connection from feature f to neuron i.

Another parameter variation D_f is defined to represent the contribution of feature f to clustering. It is derived from the related encoded feature parameter A_f^c as follows:

$$D_f = \frac{1}{k}\sum_{c=1}^{k}[A_f^c - \overline{A_f}]^2 \quad f=1,2,...,p, \tag{4}$$

where

$$\overline{A_f} = \frac{1}{k}\sum_{c=1}^{k} A_f^c \quad f=1,2,...,p. \tag{5}$$

The contribution of each feature to clustering can be evaluated by D_f. If a feature has a greater influence on clustering, its variation will be a higher value than others. Given a threshold ϵ the feature will be eliminated if its variation is less than ϵ. Otherwise, the features will be ranked in a definite sequence. Therefore, the contribution of each feature to clustering can be represented by its position in the sequence.

The procedure of feature encoding by the encoder network is described as follows:

1. Extract a set of input data, $\mathbf{X}=\{\mathbf{x}_1,\mathbf{x}_2,\mathbf{x}_t,\ldots,\mathbf{x}_n\}^T$, where each sample $\mathbf{x_t}$ consisting of p-dimensional feature vector $\mathbf{x_t}=\{f_1,f_2,...,f_p\}^T$, from a set of multispectral images.
2. Calculate the distance $\mathbf{D}_i = d(x^n, w_i)$ for all output neurons.
3. Determine the output neuron with the minimal distance as the winner i^*. Adjust the weight vectors of the winner and those of its neighbor neurons N_t as below:
   $$u_i(t) = u_i(t-1) + M_i^t, \tag{6}$$
   $$w_{ij}(t) = w_{ij}(t-1) + \frac{M_i^t}{u_i(t)}[x_i^t - w_{ij}(t-1)], \tag{7}$$
   where $M_i^t = 0$ or 1, specify whether or not an input vector $\mathbf{x^n}$ allows a weight update to neuron i in the winner's neighborhood.
4. Repeat Steps 2 and 3 until the network converges.
5. Determine the number of regions k in the SOFM and calculate the number of neurons in each region, $r = \{r_1, r_2, \ldots, r_c, \ldots, r_k\}$. Calculate the encoded feature parameter A_f^c and the variation D_f by Eqs. (3) and (4).
6. Obtain the definite sequence $Fcod(\mathbf{X})$. Determine which feature is to be eliminated or encoded from the original feature vectors according to the given threshold and then get the encoded feature vectors.

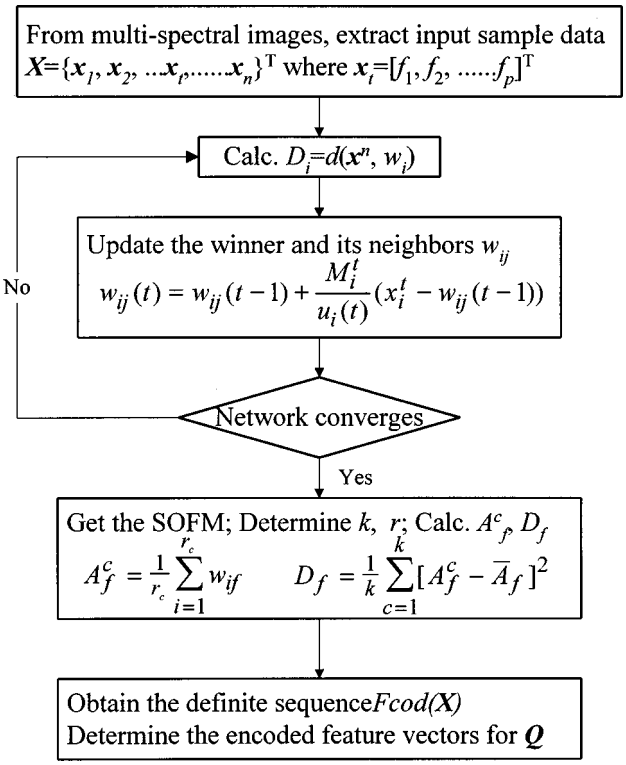

Fig. 3 The procedure of feature encoding from multispectral images.

The above procedure of feature encoding from multispectral images is illustrated in Fig. 3.

2.2 *Segmentation by Encoded Feature-Based FCM Algorithm (EFFCM)*

Although, the Approximate FCM (AFCM) algorithm and semisupervised FCM algorithm have been proposed for developing the FCM algorithm, there are some problems to be solved.[14,15] At present, there has not been a satisfactory computational solution. When c, p, and n become large, the FCM is time-consuming. Although lookup table approximations, replacing the exponent in equations of the membership u_{ik} and the center of each cluster v_i, were used to reduce the complexity of the AFCM algorithm, the optimization problem, i.e., the fuzzy c-means function J_m was not rigorously identified. The round-off method in the AFCM approach made the fuzzification parameter m change slightly at each iteration. The user must also participate to assess the segmentation. In addition, it is necessary in the methods used to specify c, the number of classes to be segmented.

Based on encoded feature vectors, the EFFCM algorithm developed for the final segmentation can optimize the conventional FCM algorithm in two aspects. One is to reorganize the original feature vector as the encoded feature vector for constituting each one of the sample data through verifying the contribution of each feature to clustering using the definite sequence. Another is to determine the number of clusters c automatically. The initial number of clusters c_0 is obtained according to the number of regions in the SOFM. By increasing and decreasing the number of clusters c within a small neighborhood, several segmentation results can be obtained. The final segmentation can then be obtained by evaluating the segmentation.

The EFFCM algorithm utilizes the fuzzy membership function to show the clustering result. The fuzzy membership function is derived in the form of a matrix $\mathbf{U}$ where the degree of each sample $\mathbf{x_k}$ belonging to class i is presented by u_{ik}. The clustering result can be obtained by applying the maximum membership rule as follows:

$$u_{ik}^{MM}=\begin{cases}1, & \text{if } u_{ik}\geqslant u_{jk} \quad j=1,2,\ldots,c;\ j\neq i \\ & \qquad\qquad i=1,2,3,\ldots c;\ k=1,2,3,\ldots,n. \\ 0, & \text{otherwise.}\end{cases} \tag{8}$$

In other words, the sample of $\mathbf{x}_k$ is assigned to cluster i when the fuzzy membership function u_{ik} achieves a larger value than others. This scheme for segmentation can be referred to as the Unsupervised Labeled Maximum Likelihood (ULML) method. The final result is represented as a pseudocolor image. The procedure of the final segmentation by EFFCM algorithm can be described as follows:

1. Reorganize the sample data set $\mathbf{X}$ as $\mathbf{Q}$, where $\mathbf{Q}=\{\mathbf{q}_1,\mathbf{q}_2,\ldots,\mathbf{q_k},\ldots,\mathbf{q_n}\}^T$, $\mathbf{q_k}=[f_1,f_2,\ldots,f_q]^T$, $q<p$. Determine the initial number of cluster c_0 as the number of regions k in SOFM.
2. Set the matrix $\mathbf{A}$, the beginning of iteration, $t=0$, and the error parameter, $\epsilon>0$. Choose the fuzzification parameter $m>1$. Assume the center of each cluster $\mathbf{V}^0=\{\mathbf{v}_1,\mathbf{v}_2,\mathbf{v_i},\ldots,\mathbf{v_c}\}$ to be random values, where $\mathbf{v_i}=[v_1,v_2,v_k,\ldots,v_q]$ and v_k refers to the value in feature vector f_k.
3. During t iteration, calculate the distance between $\mathbf{q_k}$ and $\mathbf{v_i}$,

$$D_{ik}^t=\|q_k-v_i^t\|_A, \quad \text{for } k=1,2,\ldots,n \quad \text{and } i=1,2,\ldots,c. \tag{9}$$

Let $\mathbf{I}=\{i\in\mathbf{I}|D_{ik}=0, 1\leqslant i\leqslant c\}$ calculate the fuzzy membership function represented by the matrix $\mathbf{U}$ using the following rules:
If $\mathbf{I}=\phi$, then

$$u_{ik}^t=\left(\sum_{j=1}^{c}\left(\frac{D_{ik}^t}{D_{jk}^t}\right)^{2/(m-1)}\right)^{-1},$$
$$i=1,2,3,\ldots c;\ k=1,2,3,\ldots n. \tag{10}$$

If $\mathbf{I}\neq\phi$, then $u_{ik}^t=0$ for all $D_{ik}\neq 0$; $u_{ik}^t=1$ for all $D_{ik}=0$.

4. Update the center of each cluster v_i using

$$v_i^t=\frac{\sum_{k=1}^{n}(u_{ik}^{t-1})^m x_k}{\sum_{k=1}^{n}(u_{ik}^{t-1})^m}, \quad i=1,2,3,\ldots,c, \tag{11}$$

and update D_{ik}^t and u_{ik}^t using Eqs. (9) and (10).

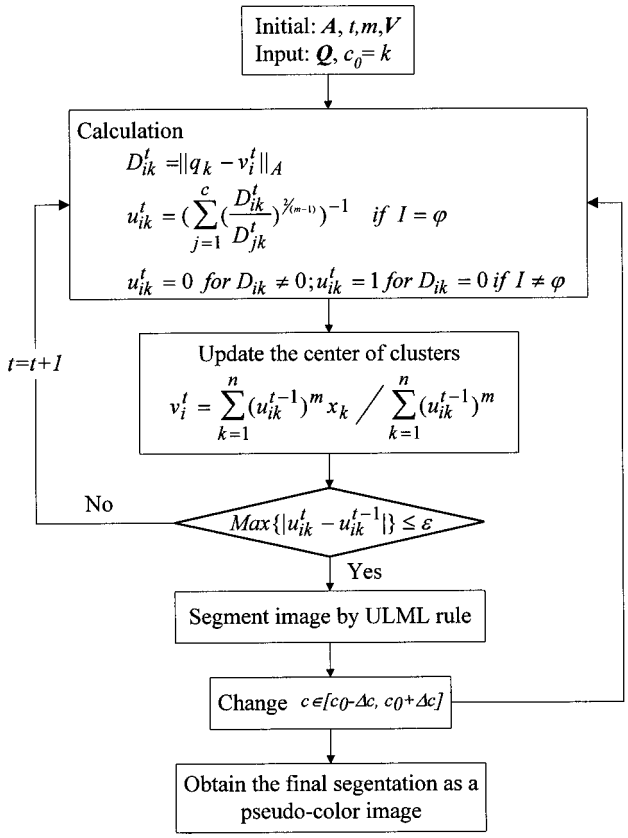

Fig. 4 The segmentation procedure of the EFFCM algorithm.

5. If $\max\{|u_{ik}^t - u_{ik}^{t-1}|\} \leq \epsilon$, stop the iteration of clustering, otherwise continue to do Steps 3 and 4.
6. Obtain the pseudocolor image by labeling the final segmentation result using ULML rule (8).
7. Given Δc, change c within the set range, $c \in [c_0 - \Delta c, c_0 + \Delta c]$, do Steps 2 through 6. Determine the final result according to the evaluation of the segmentation.

The above procedure of the final segmentation is also illustrated in Fig. 4.

3 Application of the ESNN to MR Brain Images

In MR brain image studies, the quantities of concern include the volumes of white matter, gray matter and cerebrospinal fluid (CSF). In the abnormal case, the quantitative analysis also includes precise delineation of tumors for monitoring the tumor size, growth rate, and architecture for the determination of the optimal radiation. It is obvious that MRI quantitative analysis depends heavily on the efficiency of image segmentation. MR brain image segmentation aims at assigning a set of meaningful regions to a number of tissues or organs through a set of a multispectral MR brain images. Thus, this problem concerns two aspects: segmenting the image into the classified regions and assigning a meaningful label representing a tissue or organ to each region. Here, the proposed ESNN was applied[16] for automatically labeling brain tissues in MRI.

3.1 *Experiment Descriptions*

The three-dimensional brain image data obtained from an MRI scanner consist of a stack of cross-sectional images. The image characteristics depend on the repetition time (TR) and the echo time (TE) used in scanning. Usually, a long TR is larger than 1500 s and a short TE is less than 30 s. A PD image is obtained using the long TR and the short TE. A T2-weighted image is obtained using the long TR and the long TE. In all the other cases, the obtained images are called T1-weighted images. In this experiment, the T1-weighted image is obtained with TR=480 s and TE=15 s. The PD image is obtained with TR=3000 s and TE=17 s, whereas the T2 weighted image is obtained with TR=3000 s and TE=119 s.

Seven low-level feature parameters[17] on MR brain images were used to analyze their contributions to segmentation through the feature encoder in the ESNN. For each set of multispectral MRI, there are three basic features: T1, PD, and T2 density, which can be obtained directly from the T1_weighted and T2_weighted and PD images (Figs. 5 and 6). The other features, PDT2_ratio, PDT2_gradient, PDT2_deviation, and T2_gradient need to be calculated from these images.

The experiments on the ESNN were conducted using four brain MRI for different objects. Of these, two MRI, br3 and br0 in Figs. 5(a) and 5(b), are the normal brain MRI of a male volunteer. The other two MRI, br1 and br2

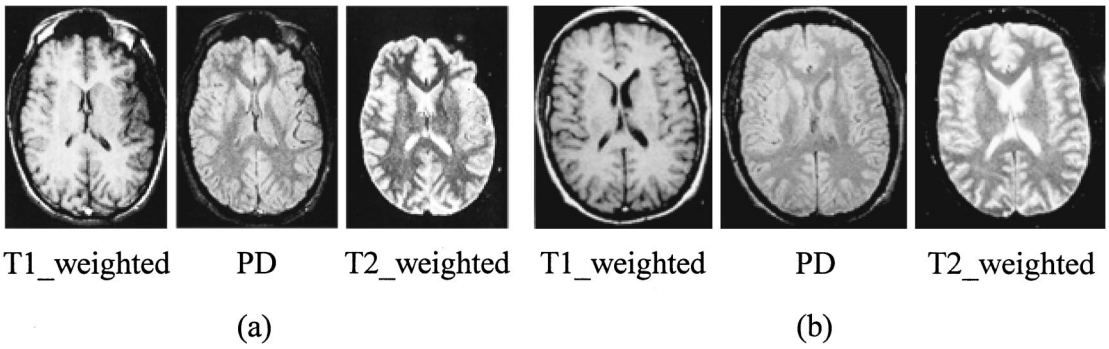

Fig. 5 An example of a normal brain MRI: (a) br3 MR images (128×92); (b) br0 MR images (128×94).

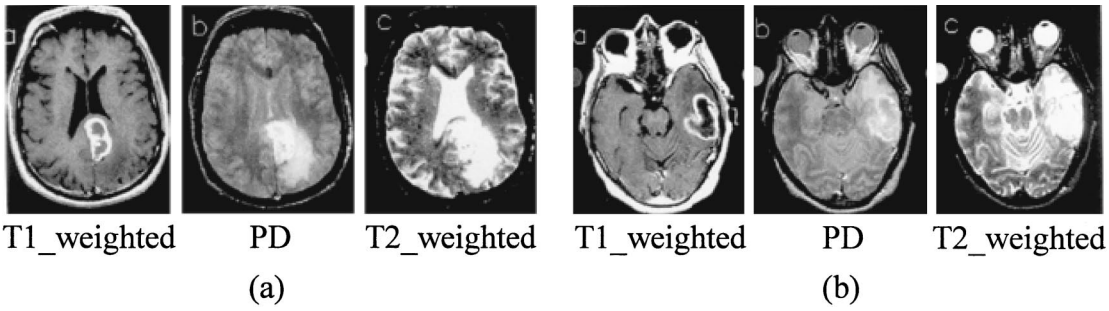

Fig. 6 An example of an abnormal brain MRI. (a) br1 MR images (128×102); (b) br2 MR images (128×104).

in Figs. 6(a) and 6(b), are of an abnormal brain MRI with tumors. From br0, br1, br2, and br3, setting the receptive field, $R=2\times1$, we extracted respectively a set of sample data 6784, 6528, 6656, and 5888, for our computation in the beginning. In the encoder network, seven neurons constitute the input layer and 100 neurons constitute the output that is constructed as a 2-D space map with 10×10 neurons. The input, a set of sample data for feature encoding, is constructed as an $n\times7$ integer value matrix whose row vector consists of seven features associated with a pixel. The weights associated with the connections from each neuron between the input layer and the output layer is constructed as a 100×7 matrix.

With the EFFCM algorithm for the final segmentation, the initial number of clusters c_0 can be determined as the number of regions k in the SOFM. The initial vectors of the center of clusters are set to random values. We then fix a positive definite matrix **A**, reflecting the relationship between the feature and the center of the clusters, as an identity matrix. A value $\epsilon=0.001$ was used as the threshold for judging the convergence of EFFCM. The EFFCM algorithm was run using different values of parameter m ranging from 1.5 to 2.0. Depending on the defuzzification method, each pixel is then uniquely assigned to the class that has the maximum membership function. It is simple to replace $\mathbf{u_k}$ by the basis vector $\mathbf{e_i}\in N_c$ for which $u_{ki}>u_{kj}$, $1\leqslant j\leqslant c$, $j\neq i$. Each pixel is then assigned a color code representing the specific tissue to which it belongs. The representation of the color code is: air (green), fat (blue), white matter (light gray), gray matter (rose), CSF (red), and tumor (dark gray). For the complex patient MRI labeling, we added the color codes: dark gray for eye organ and white for tumor or edema.

3.2 *Analysis of Feature Contributions*

The experiment results of the feature maps on br0 through br3 MRI images are shown in Figs. 7–10. As mentioned above, neurons having similar characteristics will be pulled into a group or region in the SOFM. The output with the range from 0.1 to 0.4 indicates its neuron is between the states of no activity and temporary. The output ranging from 0.6 to 0.9 indicates its neuron is between the states of temporary and activity of which the neuron has certain probability to be clustered into a group with its neighbors. Obviously, a threshold value for each region boundary should be 0.5, representing that the neuron is in the temporary state, subject to a tolerance of ±0.1. The region map is then determined where the number of regions in the SOFM k of br0, br1, br2, and br3 is 4, 6, 6, and 5, respectively. The initial number of clusters c_0 is also determined as the number of regions k. According to the output of SOFM and the set weights when the network converges, the corresponding encoded feature parameters A_f^c and the variation of each feature D_f can be calculated as shown in Tables 1–4. (Note the Representation of feature code: $f1$: T2_Gradient; $f2$: PDT2_Gradient; $f3$: T1_Density; $f4$: PDT2_Ratio; $f5$: T2_Density; $f6$: PDT2_Deviation; $f7$: PD_Density.)

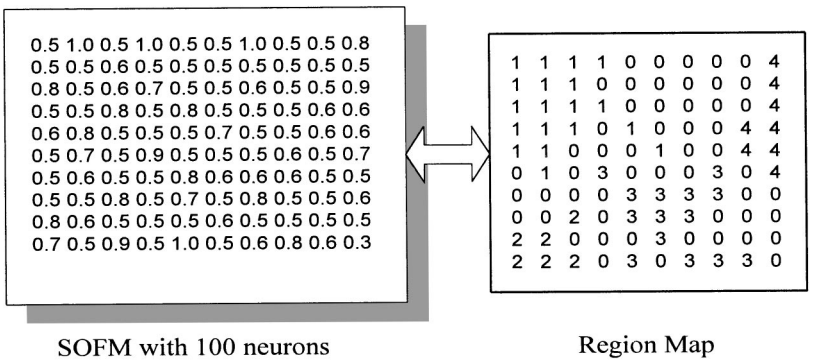

Fig. 7 Feature map of br0 MRI.

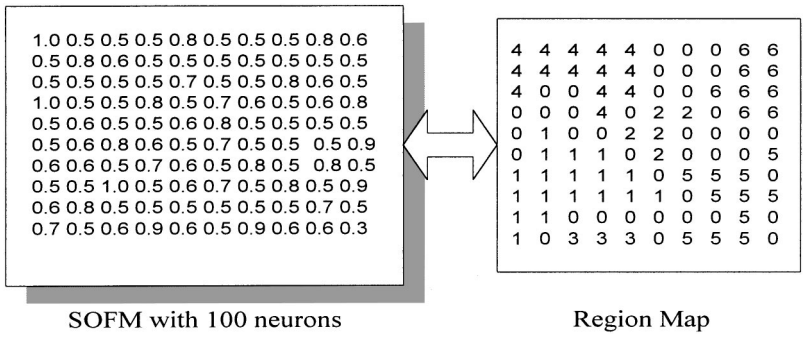

Fig. 8 Feature map of br1 MRI.

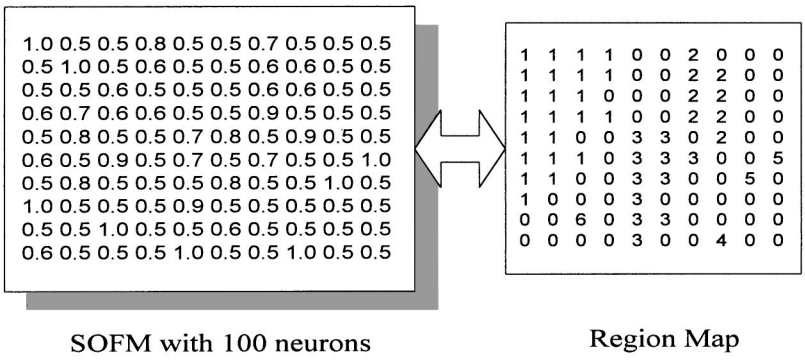

Fig. 9 Feature map of br2 MRI.

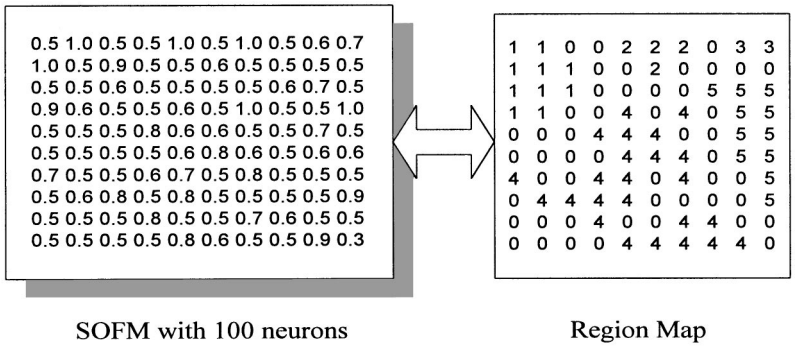

Fig. 10 Feature map of br3 MRI.

Table 1 The br0 feature encoded parameters by SOFM on 100 neurons.

br0	A1	A2	A3	A4	A_	D
*f*1	107.78	141.21	161.34	9.35	104.92	**3410.73**
*f*2	110.04	138.26	124.22	37.37	102.47	**1512.17**
*f*3	143.80	133.08	93.29	70.45	110.15	879.65
*f*4	40.41	42.95	14.02	0.97	24.59	314.26
*f*5	64.10	219.58	240.79	35.28	139.94	**8304.63**
*f*6	20.05	15.02	45.06	34.62	28.69	141.16
*f*7	59.49	78.74	219.62	283.38	160.31	**8870.93**

Table 2 The br1 feature encoded parameters by SOFM on 100 neurons.

br1	A1	A2	A3	A4	A5	A6	A_	D
*f*1	68.06	53.10	138.70	1.46	140.73	170.55	95.43	**3489.59**
*f*2	65.67	80.69	105.80	11.85	131.83	147.25	90.52	**2010.36**
*f*3	81.02	138.09	97.07	78.37	97.01	117.00	101.43	428.95
*f*4	6.44	7.95	40.91	0.94	71.77	46.06	29.01	666.96
*f*5	329.58	108.11	518.94	28.56	347.43	82.84	235.91	**3679.33**
*f*6	55.80	44.80	58.08	10.78	27.72	31.68	38.14	275.45
*f*7	386.43	244.71	297.59	89.49	124.48	79.77	203.74	**13094.23**

Table 3 The br2 feature encoded parameters by SOFM on 100 neurons.

br2	A1	A2	A3	A4	A5	A6	A_	D
*f*1	193.34	26.11	78.72	93.96	27.89	166.76	97.80	**4048.18**
*f*2	149.22	33.40	109.10	47.82	29.66	135.19	84.06	**2388.00**
*f*3	114.99	109.66	159.73	86.97	94.53	124.08	114.99	552.78
*f*4	15.35	9.01	13.43	6.71	3.31	22.06	11.65	37.70
*f*5	148.48	76.34	258.83	625.65	275.58	373.45	293.06	**31071.44**
*f*6	53.27	15.32	66.54	83.10	30.60	53.91	50.46	495.48
*f*7	132.86	127.66	326.07	484.45	220.01	238.03	254.84	**15057.73**

Based on the variation indicator, the encoded definite sequence is obtained as follows:

br0: $F_{cod}=\{f7,f5,f1,f2,f3,f4,f6\}$;

br1: $F_{cod}=\{f5,f7,f1,f2,f4,f3,f6\}$;

br2: $F_{cod}=\{f5,f7,f1,f2,f3,f4,f6\}$;

br3: $F_{cod}=\{f5,f7,f1,f2,f3,f4,f6\}$.

There are three levels for each feature in the encoded definite sequence according to the distribution of the deviation: Features with T2_density ($f5$) and PD_density ($f7$) belong to the high level. Features with T2_gradient ($f1$) and PDT2_gradient ($f2$) belong to the middle level. Features with T1_density ($f3$), PDT2_ratio ($f4$), and PDT2_deviation ($f6$) belong to the low level. The distance between any two levels is more than 1250. To analyze each feature's contribution to clustering further, the features at each level are considered as input feature vectors.

A set of sample data are then reorganized with these feature vectors $\mathbf{x_k}(h)=[f5,f7]$, $\mathbf{x_k}(m)=[f1,f2]$, and $\mathbf{x_k}(l)=[f3,f4,f6]$ to be used for segmenting the normal MRI br0 and the abnormal MRI br1. From the experimental results in Fig. 11, it is seen that utilizing feature vectors $\mathbf{x_k}(h)$, we obtain satisfactory segmentation results because the tissues and tumor were successfully separated from each other in br0 and br1. The feature vectors $\mathbf{x_k}(m)$ can affect the segmentation to a certain extent via edge information extracted. However, its influence is insignificant because it is insensitive to region information. In contrast, the feature vectors $\mathbf{x_k}(l)$ have little effect on segmentation because the segmentation failed to process the desirable regions. Furthermore, using all seven features indiscriminately in the segmentation, we found that the results are unsatisfactory from both the normal and abnormal cases. The reason is that the introduction of features $f3$, $f4$, and $f6$ has an adverse influence on the segmentation.

Table 4 The br3 feature encoded parameters by SOFM on 100 neurons.

br3	A1	A2	A3	A4	A5	A_	D
*f*1	3.24	31.04	101.52	144.59	159.15	87.91	**3775.13**
*f*2	5.01	25.88	70.41	136.44	134.92	74.53	**2939.33**
*f*3	16.02	29.14	50.56	148.75	137.57	76.41	3104.94
*f*4	2.10	11.16	20.00	25.82	76.93	27.20	682.86
*f*5	15.90	381.36	748.55	212.88	567.87	385.31	**6629.66**
*f*6	4.58	14.11	61.62	40.44	45.10	33.17	437.08
*f*7	29.92	76.16	322.12	165.27	240.63	166.82	**11306.04**

The experimental results confirmed the above feature encoded definite sequence. Thus, the encoded features can provide the quantitative indicator to rank the features so that the algorithm can correctly guide the postsegmentation by using the meaningful feature vectors.

After extracting the features by the feature encoder network, features T2_density ($f5$) and PD_density ($f7$) are then reorganized as the encoded feature vectors for the final segmentation by the EFFCM algorithm.

3.3 *Experimental Results and Evaluations*

To verify the validity of the ESNN-based method, tests were conducted on simulated data. In the test image, we used four different vertical stripes to represent the regions of CSF, white matter, gray matter, and tumor of an MR brain image, as shown in Figs. 12(a), 12(b), and 12(c). The first three strips were designed to simulate the CSF and white and gray matter structures with distinct intensity values. For example, in Fig 12(a), the CSF, and white and gray matter were set at 10, 150, and 120, respectively, in the T1 image. The fourth strip was chosen to represent tumor whose intensity values are usually over 200 in T1, T2, and PD images. Using the ESNN-based method, the computed mean intensity of each tissue class was found to be the same as the true mean intensity of the simulated image stripes. The success of our method can be seen in Fig. 12(d).

Next, experiments were performed on some real MR images. The segmentation results of br0, br1, br2, and br3 using the ESNN approach are shown in Fig. 13(a) through 13(d). To demonstrate the advantage of the ESNN method, the FCM algorithm is implemented for segmenting br0 through br3 MRI with the results shown in Fig. 14(a) through 14(d).

The performances of the two algorithms on the normal volunteers and the tumor patients were then studied. The results by the ESNN and the FCM method both yielded ''correct'' segmentation. Evaluating these segmentations further, the ESNN results showed improvements over the FCM method because the ESNN can distinguish the main

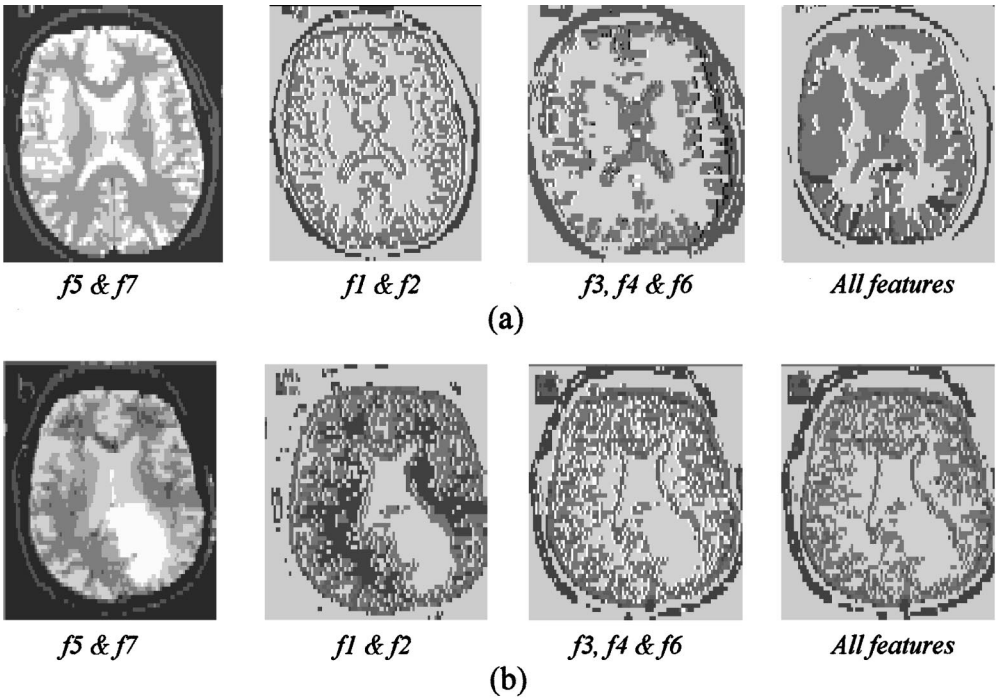

Fig. 11 Feature influence on br0 (a) and br1 (b) segmentation by clustering.

tissues such as white matter (light gray), gray matter (rose), and CSF (red) exactly and entirely in terms of anatomy. In contrast, the FCM results did not seem to convey enough details and partly mixed gray matter with CSF in some regions. This can be seen, for example, in the results of labeling on br0 MRI as given in Figs. 13(b) and 14(b). Furthermore, for the case of the patient study, the ESNN method gives better results compared with the FCM method for segmenting MR images. Figure 13(c) shows that tumor in br1 can be distinguished from the surrounding tissues, i.e., CSF and gray matter with a distinct boundary. Figure 14(c) shows that the tumor's boundary had some faults due to the tendency toward the upper boundary between CSF and gray matter although the tumor is also separated from the surrounding tissues. For the br2 MRI, when c increased to 7 using the ESNN method, Fig. 13(d) shows that part of the eye (dark gray) can be distinguished from the tumor (white). This was not achievable with the tumor using the FCM method shown in Fig. 14(d). However, using the ESNN method, some part of the fat is mixed with air on the boundaries. This is not a main concern in segmenting brain tissues. What is most important is whether the main tissues could be separated accurately from the background and from each other.

To show the effectiveness of the ESNN-based method, its segmentation results were compared with those of FCM for brain MR images. In this experiment, we first chose three types of tissues for quantitative evaluation: CSF, white matter, and gray matter. For each method, we computed two center values of each feature. One (Clst. Cent) is computed by the algorithm. The other (Result Cent) is the mean value of the region of the tissue from the final labeling result obtained by the corresponding method. Finally, we computed the standard deviations and the percent changes in the standard deviations for each method. The percent change is obtained by subtraction of the standard deviation of the FCM method from that of the ESNN method divided by that of the FCM method. The results are given in Tables 5–8.

The results show a global reduction in the standard deviation for the ESNN method compared to the FCM method, especially for the case of the br1 image. In terms

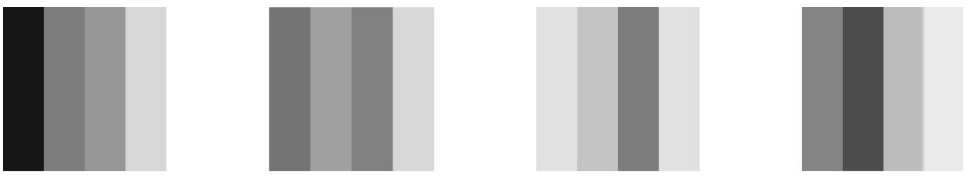

Fig. 12 Evaluation results where (a), (b), and (c) are the simulated data with stripes left-to-right showing CSF, gray matter, white matter, and tumor in T1, PD, and T2 images and (d) shows the final segmentation result by the ESNN method.

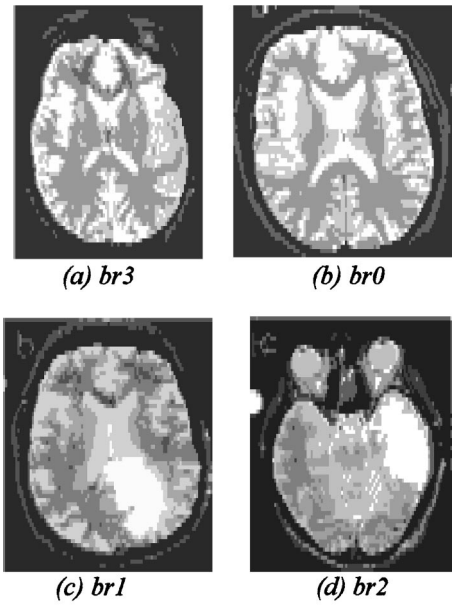

Fig. 13 Results by the ESNN.

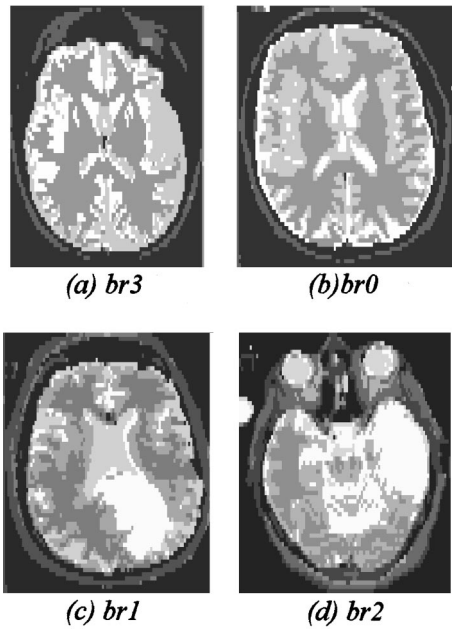

Fig. 14 Results by the FCM.

Table 5 Quantitative comparison for brain MRI br0 through br3: CSF.

	ESNN			FCM			
Slice	Clst. Cent	Result Cent	Deviation	Clst. Cent	Result Cent	Deviation	Change of Deviation %
	201.3	202.0	1.20	188.3	186.0	1.88	−35
br0	148.1	145.9		123.0	118.8		
				47.6	44.6		
	205.8	204.7	1.55	203.4	198.8	2.07	−25
br1	136.0	133.1		142.1	138.7		
				30.5	28.1		
	27.9	28.9	1.77	12.6	14.0	2.42	−31
br2	83.8	87.2		64.4	71.4		
				214.7	216.0		
	164.1	166.1	4.27	190.2	190.4	3.33	+28
br3	145.9	137.6		140.4	132.4		
				87.1	81.1		
Average			2.198			2.425	−9.4

Table 6 Quantitative comparison for brain MRI br0 through br3: gray matter.

	ESNN			FCM			
Slice	Clst. Cent	Result Cent	Deviation	Clst. Cent	Result Cent	Deviation	Change of Deviation %
	156.6	156.5		175.8	177.3		
br0	143.9	144.2	0.15	151.7	151.5	0.51	−71
				126.7	126.4		
	134.0	135.4		140.7	144.5		
br1	123.4	122.4	0.86	124.9	125.5	1.29	−33
				117.7	117.4		
	116.5	122.6		92.5	89.2		
br2	93.8	90.1	3.56	109.8	113.5	3.70	−3.8
				140.9	147.1		
	209.7	212.7		188.2	190.7		
br3	176.9	178.5	1.70	172.3	174.8	1.64	+3.7
				167.4	170.8		
Average			1.568			1.77	−11

Table 7 Quantitative comparison for brain MRI br0 through br3: white matter.

	ESNN			FCM			
Slice	Clst. Cent	Result Cent	Deviation	Clst. Cent	Result Cent	Deviation	Change of Deviation %
br0	119.2	118.3		122.2	122.4		
	120.9	120.2	0.57	126.3	127.2	0.45	−27
				153.0	152.0		
br1	16.2	15.4		4.5	6.3		
	78.9	78.9	0.40	18.2	23.8	2.13	−81
				175.9	178.4		
	145.3	145.0		147.6	148.7		
br2	135.3	138.8	1.76	134.6	136.4	1.48	+19
				132.1	136.0		
	103.7	103.5		102.1	103.1		
br3	129.8	129.9	0.11	131.1	131.8	0.95	−88
				183.8	181.2		
Average			0.928			1.268	−27

of percent change in the standard deviation, the ESNN method improves on the FCM method by nearly 31%:

$$\left(\frac{9.4+11+27+78}{4}\%=31\%\right).$$

In particular, the case of the tumor shows that the ESNN method outperforms the FCM method in abnormal cases. From Table 8, we found that the ESNN method improved greatly on the FCM method by 78% in the average value of deviation.

Uniformity is another measure normally adopted for quantitative evaluation of segmentation results.[18] Uniformity of a feature over a region is inversely proportional to the variance of the values of that feature evaluated at every pixel in that region. Our uniformity evaluations were conducted on a series of segmented image pairs obtained by the ESNN-based method and the FCM method. From the results, we found that using the ESNN-based method, a uniformity value as high as 0.997 is achievable, which proves satisfactory in practical applications. This quantitative result and those from the tables in the above experiments confirm the qualitative impression we asserted from the segmented images.

In terms of computation time, our ESNN method consumes different times for segmenting the normal and abnormal MR images. In this experiment, we used Visual C++ for implementing our ESNN method on a Pentium 100 with 32-Mb memory. Using the ESNN method, it took about 25 min for the normal case and about 40 min for the abnormal case. In contrast, when using the FCM algorithm, it took about 30 min for the normal case and about 1 h for the abnormal case. Because the original data from the MR brain images were compressed first by the receptive field and then the feature vectors were further encoded by the encoder network, our ESNN method is computationally more efficient than the FCM algorithm.

Because the user will not have any prior knowledge of the number of clusters, it is impossible to automate the segmentation completely. The EFFCM algorithm obtains the initial number of clusters by the SOFM during the training of the encoder network and then varies the number of clusters with the given Δc value for clustering until the best segmentation is achieved. For example, from the region maps in br0 and br1 in Figs. 7 and 8, the initial number of clusters c_0 is 4 and 6. Let Δc be ± 2. Figure 15 shows an alternative processing method for finding the best number of clusters 5 and 7, respectively, based on the evaluation of the results of segmentation. It was found that the EFFCM algorithm would converge to meaningful clusters for normal MRI cases with five cluster centers and for abnormal MRI cases with six to seven cluster centers. Finding the right number of clusters is an important problem known as the cluster validity problem.[19–21] Because the final number

Table 8 Quantitative comparison for brain MRI br0 through br3: tumor.

	ESNN			FCM			
Slice	Clst. Cent	Result Cent	Deviation	Clst. Cent	Result Cent	Deviation	Change of Deviation %
	227.6	226.1		221.3	222.8		
br1	216.1	215.5	0.39	193.2	191.5	2.96	−87
				120.2	128.8		
	234.2	234.0		210.8	215.0		
br2	190.3	191.7	0.71	165.3	168.2	2.10	−66
				121.6	124.7		
Average			0.55			2.53	−78

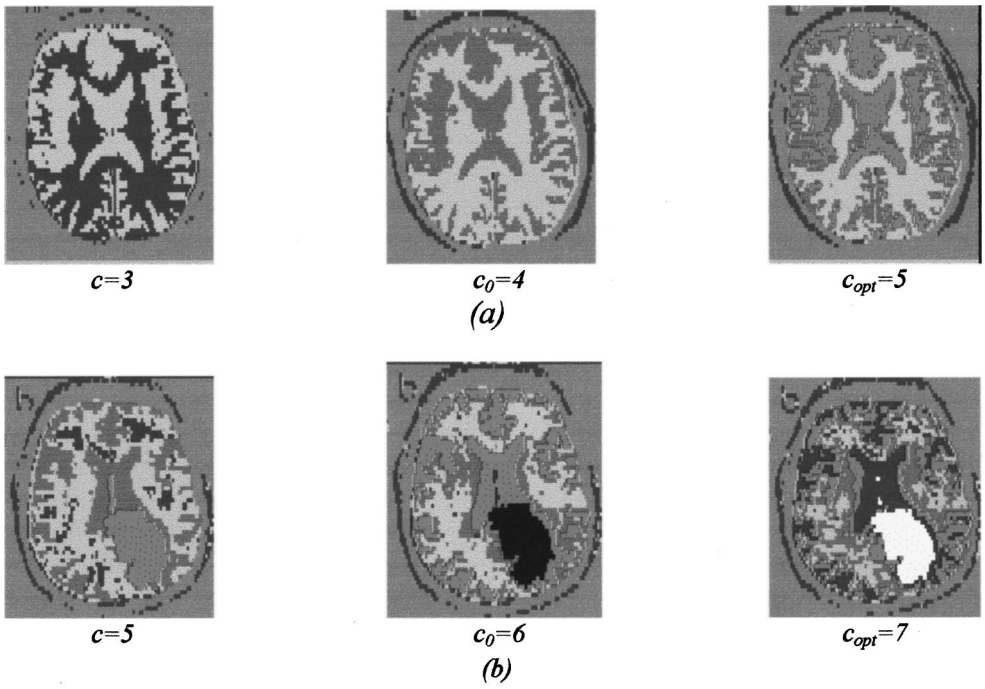

Fig. 15 An alternative procedure for finding the number of clusters: (a) br0 and (b) br1.

of clusters is determined through the best results obtained by experience, a further work is to improve fuzzy clustering for pattern recognition with applications to image segmentation by using the ESNN approach.

4 Conclusion

The key factor to the success of MRI segmentation is the development and optimization of pattern recognition methods that have the best potential for segmentation. Statistical approaches toward automatically classifying tissues in MRI are based on the determination of the number of classes and the extraction of feature vectors converted from the multispectral MRI. Any parameter requiring extensive user interactions should be avoided.

In this paper, a new ESNN-based approach is taken for adaptive segmentation of multispectral images. The SOFM is utilized to analyze the selected features to arrive at a suitable feature vector for improving the performance of segmentation. The EFFCM algorithm reduced the amount of sample data. Using the EFFCM algorithm, we can improve the performance of existing FCM algorithms for feature extraction and automatic cluster number determination. Quantitative evaluations and comparisons with other methods show that the developed ESNN method outperforms the FCM algorithm method by about 31% in segmenting MR brain images. With the ESNN method, satisfactory performance is achieved in the uniformity measurement. The computation efficiency achieved is higher compared with conventional clustering approaches, which is particularly important when processing a large number of patterns in multidimensional feature vectors.

Acknowledgment

This work received support from the Research Grants Council of Hong Kong through Grant Number 9040368.

References

1. N. R. Pal and S. K. Pal, ''A review on image segmentation techniques,'' *Pattern Recogn.* **26**(9), 1277–1294 (1993).
2. J. C. Bezdek, L. O. Hall, and L. P. Clarke, ''Review of MRI segmentation techniques using pattern recognition,'' *Med. Phys.* **20**(4), 1033–1046 (1993).
3. M. W. Vannier, R. G. Levitt, R. L. Butterfield, M. Gado, and D. Jordon, ''Multispectral analysis of magnetic resonance image,'' *Radiology* **154**, 221–224 (1985).
4. M. W. Vannier, C. M. Speidal, and D. L. Rickman, ''Magnetic resonance imaging multi-spectral tissue classification,'' *NIPS* **3**(2), 1182–1186 (1991).
5. L. P. Clarke, R. P. Velthuizen, L. O. Hall, J. C. Bezdek, A. M. Bensaid, and M. Silbiger, ''Comparison of supervised pattern recognition techniques and unsupervised methods for MRI segmentation,'' *Medical Imaging VI, Proc. SPIE* **1652**, 668–677 (1992).
6. H. Ball and D. J. Hall, ''IOSDATA, a novel method of data analysis and pattern classification,'' *Stanford Res. Inst.*, Menlo Park, CA, April (1965).
7. C. Darken and J. Moody, ''Fast adaptive *c*-means clustering: some empirical results,'' *Proc. IEEE IJCNN Vol. II*, 233–238 (1990).
8. L. O. Hall, A. M. Bensaid, L. P. Clarke, R. P. Velthuizen, M. S. Silbiger, and J. C. Bezdek, ''A comparison of neural network and fuzzy clustering techniques in segmenting magnetic resonance images of the brain,'' *IEEE Trans. Neural Netw.* **3**(5), 672–682 (1992).
9. N. Li and Y. Li, ''Image segmentation by an encoder-segmented neural network,'' *AeroSense Symposium on Signal and Image Processing, Proc. SPIE* **3384**, 177–185 (1998).
10. T. Kohonen, *Self-Organization and Associative Memory*, Springer, New York (1988).
11. A. K. Krishnamurthy, A. C. Ahalt, D. E. Melton, and P. Chen, ''Neural network for vector quantization of speech and images,'' *IEEE J. Sel. Areas Commun.* **8**(8), (Oct. 1990).
12. I. H. Liu and D. Y. Yun, ''Competitive learning algorithms for image coding,'' in *Applications of Artificial Neural Networks III, Proc. SPIE* **1709**, (1992).
13. V. Srinivasan, P. Bhatia, and S. H. Ong, ''Edge detection using a neural network,'' *Pattern Recogn.* **27**, 1653–1662 (1994).
14. K. Tanaka and M. Sugeno, ''Efficient implementation of the fuzzy

c-means clustering algorithms,'' *IEEE Trans. Pattern. Anal. Mach. Intell.* **8**, 248–255 (1986).
15. A. M. Bensaid, J. C. Bezdek, L. O. Hall, R. P. Velthuizen, and L. P. Clarke, ''A partially supervised fuzzy *c*-means algorithm for segmentation of MR images,'' *Science of Neural Networks, Proc. SPIE* **1710**, 522–528 (1992).
16. N. Li and Y. Li, ''Automatic labeling of brain tissues in MRI using an encoder-segmented neural network,'' *Applications of Digital Image Processing XXI*, A. G. Tescher, Ed., *Proc. SPIE* **3460**, 86–97 (1998).
17. S. P. Raya, ''Low-level segmentation of 3-D magnetic resonance brain images—a rule-based system,'' *IEEE Trans. Med. Imaging* **9**(3), 327–337 (1990).
18. M. D. Levine and A. M. Nazif, ''Dynamic measurement of computer generated image segmentation,'' *IEEE Trans. Pattern. Anal. Mach. Intell.* **7**, 155–164 (1985).
19. N. R. Pal and J. C. Bezdek, ''On cluster validity for the fuzzy *c*-means model,'' *IEEE Trans. Fuzzy Systems* **3**(3), 370–379 (1995).
20. N. R. Pal and J. Biswas, ''Cluster validation using graph theoretic concepts,'' *Pattern Recogn.* **30**(6), 847–857 (1997).
21. M. Ozkan, B. M. Dawant, and J. M. Robert, ''Neural network based segmentation of multi-model medical images: a comparative and prospective study,'' *IEEE Trans. Med. Imaging* **12**(3), 534–544 (1993).

Ning Li received the BSc degree in automatic control from the Nanjing University of Aeronautics and Astronautics in 1990. She is currently a Master candidate in the Department of Manufacturing Engineering and Engineering Management, City University of Hong Kong. Her research interests are digital image processing, pattern recognition, neural networks, and computer vision.

Youfu Li received the BS and MS degrees in electrical engineering from Harbin Institute of Technology, China, in 1982 and 1986, respectively. From 1989 to 1993, he worked in the Robotics Research Group, Department of Engineering Science, University of Oxford, United Kingdom. He obtained the PhD degree in engineering science from the University of Oxford in 1993. From 1993 to 1995 he was a postdoctoral research associate in the AI and Robotics Research Group in the Department of Computer Science at the University of Wales, Aberystwyth, United Kingdom. He is currently an assistant professor in the Department of Manufacturing Engineering and Engineering Management at City University of Hong Kong. His research interests include real-time sensor-based control of robot manipulators, vision-guided manipulation, and virtual reality.